DOI 10.36146/2026_10_06

Enhancing the fatigue performance of an L-PBF AlSi10Mg alloy through integrated HIP and T6 post-processing

M. Merlin, D. Maghini, C. Morales, C. Soffritti, D. Benasciutti, L. Mengoli, J. Shipley

Laser Powder Bed Fusion (L-PBF) enables the fabrication of complex AlSi10Mg components for lightweight structural applications. However, the as-built (AB) condition is characterized by process-induced defects and microstructural anisotropy that compromise fatigue performance. This study investigates the influence of two post-processing routes—hot isostatic pressing (HIP) and HIP integrated with T6 heat treatment (HIPT6)—on microstructure and rotating-bending fatigue behaviour (up to $5X10^6$ cycles) of the L-PBF AlSi10Mg alloy. The corresponding fatigue curves were estimated by a bi-conditional probability-stress-life (P–S–N) model from the literature. The results show that HIP strongly reduces process-induced internal defects, effectively increasing fatigue strength in the medium-high cycle regime. Although the HIPT6 condition exhibited higher scatter in fatigue life than that in HIP and AB conditions, it yielded superior performance at high stress amplitudes. The fracture mechanisms were investigated via SEM fractography.

KEYWORDS: L-PBF ALSI10MG ALLOY; POST-FABRICATION HEAT TREATMENTS; ROTATING-BENDING FATIGUE; MICROSTRUCTURE.

INTRODUCTION

Laser-Powder Bed Fusion (L-PBF) has already emerged as a crucial technology for the fabrication of highly complex metallic components with minimal time and material waste. In this context, the use of aluminum alloys, specifically the AlSi10Mg alloy, has become highly attractive for demanding applications in automotive, aerospace and biomedical sectors, due to its excellent corrosion resistance, high strength, and low density [1, 2]. The high thermal gradients and cooling rates inherent to additive processes generate columnar grains and a fine cellular-dendritic microstructure that enhance strength but also promotes high residual stresses and anisotropic mechanical properties [3-5]. Additionally, defects such as porosity and lack of fusion (LOF) adversely affect fatigue resistance. Regarding the fatigue behaviour of L-PBF AlSi10Mg alloy, authors such as Sausto et al. [6] focused on the effect of surface quality but also of internal defects and residual stresses on fatigue performance. A viable strategy to improve the fatigue resistance of as-built (AB) L-PBF components, beyond the careful selection of printing parameters, is the use of specific post-processing treatments—such as the hot isostatic pressing (HIP)—to optimize the microstructure. The HIP treatment reduces internal porosity and relieves residual stresses through the simultaneous application of high temperature and isostatic pressure. Specifically, Elad Uzan et al. [7] compared the fatigue life of specimens in the AB condition with those

Mattia Merlin, Davide Maghini, Cindy Morales, Chiara Soffritti
Department of Engineering (DE), University of Ferrara, Ferrara, Italy

Denis Benasciutti
Polytechnic Department of Engineering and Architecture (DPIA), University of Udine, Udine, Italy

Luca Mengoli
Il Sentiero International Campus srl, Castelvetro (Modena), Italy

Jim Shipley
Quintus Technologies AB, Vasteras, Sweden

under different HIP treatment conditions. It was observed that these post-processing heat treatments have a strong effect on the fatigue life. Furthermore, Aboulkhair et al. [8] found that combining heat treatment and high surface quality promotes far superior fatigue properties. Nevertheless, while HIP effectively closes internal pores, it also coarsens the microstructure leading to a reduced yield strength, often requiring subsequent heat treatments like T6 to restore mechanical strength.

Despite the extensive literature on the static mechanical properties of L-PBF AlSi10Mg, comparatively fewer studies have systematically examined the influence of integrated post-processing treatments on rotating-bending fatigue properties, particularly when comparing HIP and an innovative treatment—that combines the HIP process, gas quenching and ageing at high pressure—to achieve a T6-like state (HIPT6). To address this gap, the present study investigates the fatigue behaviour of L-PBF AlSi10Mg in the AB, HIP, and HIPT6 conditions. To account for experimental scatter, the fatigue data were fitted using a bi-conditional probability-stress-life (P-S-N) model. Microstructural investigations were carried out by optical microscopy (OM), while the fracture surfaces were examined using scanning electron microscopy (SEM) to establish the relationship between post-processing, fracture mechanisms, and fatigue performance.

EXPERIMENTAL PROCEDURE

Gas-atomized m4p™ AlSi10Mg powder, with nominal chemical composition of (wt.%) 9.0–11.0 Si, 0.20–0.45 Mg, Fe ≤ 0.55, Cu ≤ 0.050, Mn ≤ 0.45, Zn ≤ 0.10, Ni ≤ 0.050, Ti ≤0.15, and Al as balance, was used to fabricate specimens for tensile and fatigue testing. Specimen dimensions were selected in accordance with ASTM E8/E8M-21 and ASTM E466-15 standards. All specimens were printed via Laser-Powder Bed Fusion (L-PBF) using a SISMA MySint300 (SISMA S.p.A., Vicenza, Italy) additive manufacturing machine, perpendicularly to the building platform (along the Z-axis), and under a platform preheating temperature of 200 °C. Specimen fabrication was carried out using a laser power of 416 W, a laser speed of 1878 mm/s, a layer thickness of 30 μm, a "stripes" scanning strategy and under an Argon atmosphere. The powder morphology was characterized by SEM using a Zeiss EVO MA15 microscope (Carl Zeiss, Jena, Germany), equipped with an Oxford Xmax 50 detector (Oxford Instruments, Abingdon-on-Thames, UK), operating in secondary electron (SE-SEM) and backscattered electron (BSE-SEM) imaging (figure 1).

After printing, two different post-processing thermal routes were applied to some specimens. Three tensile and fifteen fatigue testing specimens were kept in the AB condition, while the remaining specimens were treated as described in table 1. Specifically, three tensile and fifteen fatigue specimens underwent a hot isostatic pressing (HIP) treatment consisting of a solution treatment at 520 °C for 2 h under an isostatic pressure of 170 MPa. Another set of three tensile and fifteen fatigue specimens were subjected to the same HIP parameters followed by rapid cooling and an in-vessel artificial aging at 180 °C for 4 h to achieve a T6-like state (HIPT6). The HIPT6 treatment was performed using a Quintus Uniform Rapid Quenching (URQ®) system combined with a Quintus Purus® toolbox (Quintus Technologies AB, Västerås, Sweden).

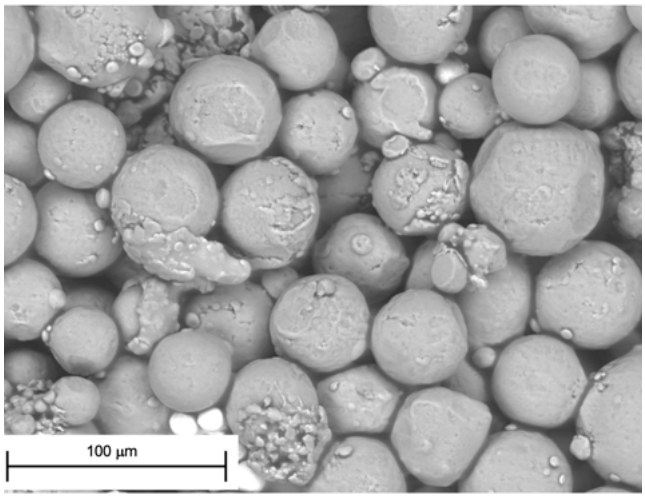

Fig.1 - BSE-SEM micrograph showing the morphology of the AlSi10Mg powder employed in this study / *Micrografia BSE-SEM in modalità elettroni retrodiffusi che mostra la morfologia della polvere in lega AlSi10Mg utilizzata in questo lavoro.*

Tab.1 - Metallurgical conditions and post-fabrication parameters of the AlSi10Mg specimens / *Condizioni metallurgiche e parametri di post-fabbricazione applicati sui campioni AlSi10Mg.*

Metallurgical condition	Type of specimen	Quantity	Post-fabrication parameters
AB	Tensile	3	-
	Fatigue	15	
HIP	Tensile	3	solution treatment @ 520 °C x 2 h @170 MPa
	Fatigue	15	
HIPT6	Tensile	3	solution treatment @ 520 °C x 2 h @170 MPa + aging x 4 h @ 180 °C @ 170 MPa
	Fatigue	15	

After fabrication and thermal treatments, all specimens were machined to reach a nominal surface finishing with Ra = 0.8 μm. Tensile tests were performed at room temperature in a Universal Galdabini Quasar 50 kN (Galdabini, Cardano al Campo, Italy) tensile machine, while the cylindrical fatigue specimens were subjected to rotating-bending fatigue tests (stress ratio R=-1) using an Italsigma RB35 (Italsigma, Forlì, Italy) electromechanical testing machine. Specifically, fatigue tests were carried out at room temperature with a rotational speed of 3000 rpm, and the run-out was settled at $5x10^6$ cycles. The experimental fatigue data were analysed using a bi-conditional probability-stress-life (P-S-N) model proposed in the literature [9]. The model introduces two distinct cumulative probability distributions: one describing the scatter of finite-life fatigue data in the inclined portion of the stress-life (S-N) curve, and the other describing the random fatigue limit in the infinite-life portion. Metallographic and fractographic characterization were subsequently conducted on samples drawn from the fractured specimens employing a Leica DMi8 A optical microscope (Leica, Wetzlar, Germany) and the same Zeiss EVO MA15 scanning electron microscope equipped with an Oxford Xmax 50 microprobe for energy-dispersive spectroscopy (EDS).

RESULTS AND DISCUSSION

Microstructure and tensile properties

The tensile testing results show that HIP strongly affects the mechanical strength of the alloy. By comparing the micrographs of figure 2a (AB) and 2b (HIP)—recorded in back-scattered (BSE-SEM) imaging—the HIP treatment leads to the disruption of the continuous eutectic Al-Si network, replaced by coarsened Si particles. Although these microstructural changes in the HIP condition reduce the yield strength (YS) and ultimate tensile strength (UTS), they are expected to improve fatigue performance by reducing internal porosity and increasing tensile ductility. The HIPT6 route, on the other hand, successfully restored mechanical strength via precipitation hardening, achieving the highest yield strength (236 MPa). While secondary Fe-rich phase is clearly visible in both post-treated conditions (see red arrows in figure 2b and 2c), the submicrometric precipitates induced by aging in HIPT6 are too fine to be resolved by SEM, resulting in a microstructure highly similar to the HIP condition. The tensile properties for the three metallurgical conditions are summarized in table 2, serving as a fundamental baseline for fatigue test design and discussion.

Tab.2 - Tensile properties of the AlSi10Mg alloy in the different metallurgical conditions / *Proprietà a trazione della lega AlSi10Mg nelle differenti condizioni metallurgiche.*

	UTS (MPa)	YS (MPa)	A%
	AB		
Mean value	387	212	4.6
Std. Dev.	4	4	0.2
	HIP		
Mean value	253	162	11.4
Std. Dev.	4	1	1.1
	HIPT6		
Mean value	387	236	7.2
Std. Dev.	3	4	0.5

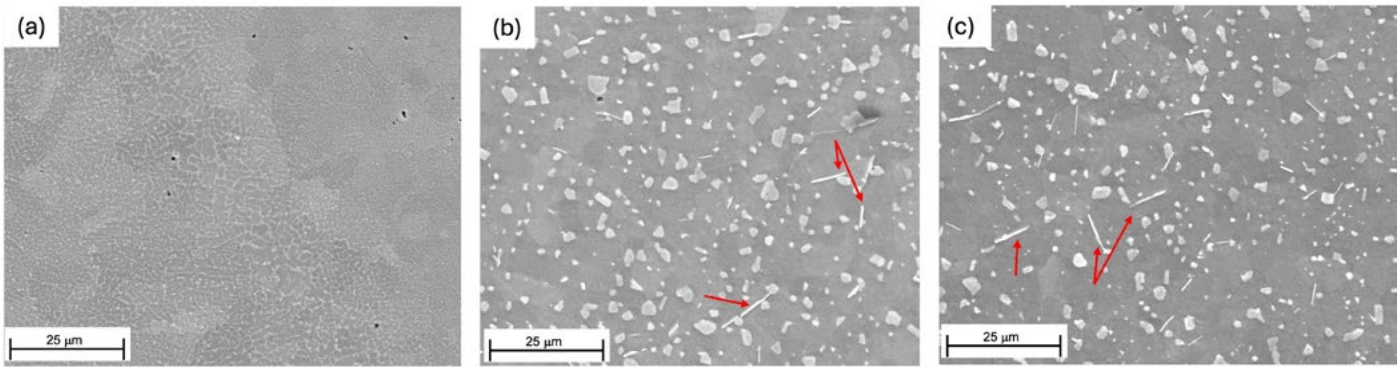

Fig.2 - (a-c) BSE-SEM micrographs of the AlSi10Mg alloy in the AB, HIP and HIPT6 conditions (Fe-rich phases are indicated by red arrows) / *(a-c) Micrografie BSE-SEM della lega AlSi10Mg negli stati AB, HIP e HIPT6 (le fasi ricche in Fe sono indicate da frecce rosse).*

Fatigue performance and fractographic analysis

The mean S-N curves for AB, HIP and HIPT6 conditions, reported in figure 3, demonstrate a clear improvement in fatigue performance after post-fabrication treatments. The AB condition exhibited the lowest fatigue resistance, with a fatigue limit of approximately 100 MPa. The HIP treatment led to an increase in the fatigue limit by approximately 49% (reaching 149 MPa), while the integrated HIPT6 treatment further raised the fatigue limit to 160 MPa, corresponding to a 60 % overall improvement compared to the AB condition. Fractographic analysis of the fracture surfaces revealed distinct initiation and propagation mechanisms. In the AB specimen, fatigue crack initiation occurred at the surface, driven by manufacturing defects as depicted in figure 4a. Observations at higher magnification (yellow insets in figure 4a) confirmed that an irregular pore associated with partially fused material acted as the preferential crack initiation site. Conversely, crack initiation in the HIP specimen (figure 4b) was triggered by un-melted powder, likely associated with a process-related lack of fusion that was subsequently closed during the HIP treatment; this defect closure explains the delayed fatigue crack nucleation and the resulting higher fatigue limit. In the HIPT6 specimen (figure 4c), a minor surface discontinuity acted as crack nucleation site. The final overload regions (figures 4d–f) also revealed peculiar differences in fracture morphology at higher magnifications. The AB specimen exhibited a relatively rough fracture surface with numerous irregular cavities associated with process-induced defects assisted by the brittle fracture of the Al-Si eutectic network. In contrast, HIP and HIPT6 specimens showed predominantly ductile fracture characterized by extensive microvoid coalescence and uniformly distributed dimples, consistent with the improved ductility measured during tensile testing.

Condition	Inverse slope, b	Fatigue limit, S_∞	Std. Dev., $\ln(\bar{N})$	Std. Dev., S_∞
AB	6.34	100 MPa	0.25	4.04 MPa
HIP	22.65	149 MPa	0.7	4.60 MPa
HIPT6	14.56	160 MPa	0.65	7.11 MPa

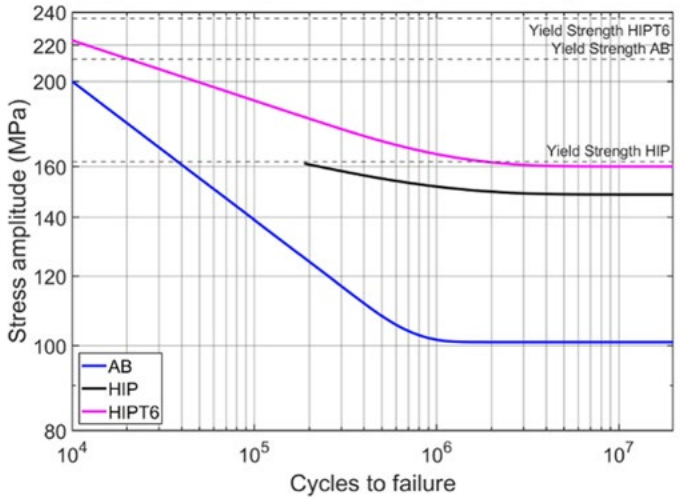

Fig.3 - S-N mean curves of L-PBF AlSi10Mg in AB, HIP and HIPT6 conditions. The upper table shows the statistical fatigue model parameters, including inverse slope, fatigue limit and standard deviations of fatigue life and fatigue limit / *Curve S-N medie della lega AlSi10Mg L-PBF nelle condizioni AB, HIP e HIPT6. La tabella mostra i parametri statistici del modello, inclusi la pendenza inversa, il limite di fatica e le deviazioni standard della vita a fatica e del limite di fatica.*

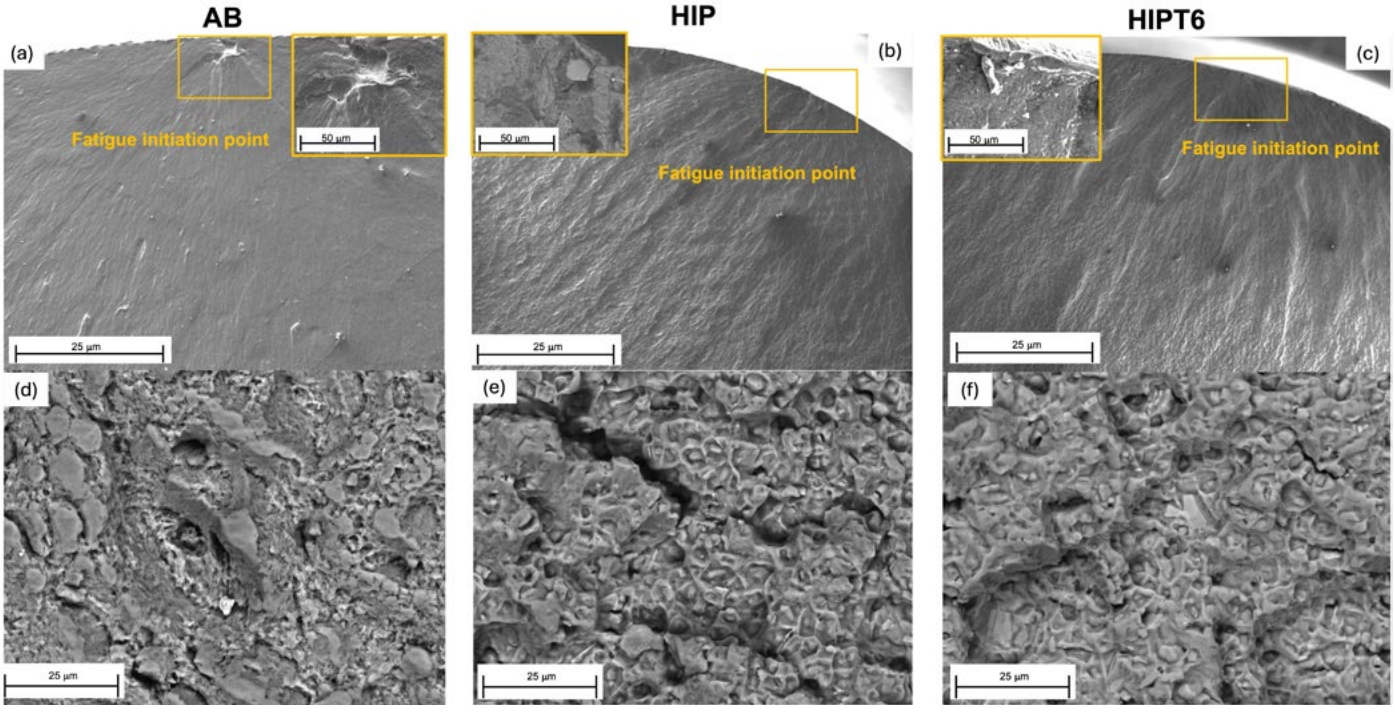

Fig.4 - SE-SEM micrographs of fracture surfaces of fatigue specimens. (a–c) Fatigue crack initiation regions for AB, HIP and HIPT6 specimens, respectively. Yellow insets provide higher-magnification images of the initiation defects. (d–f) Higher-magnification SE-SEM micrographs of the overload fracture regions for corresponding AB, HIP and HIPT6 specimens / *Frattografie SE-SEM dei provini di fatica. (a–c) Regioni di innesco della cricca di fatica rispettivamente per i provini AB, HIP e HIPT6. I riquadri gialli forniscono un ingrandimento dei difetti di innesco. (d–f) Micrografie SE-SEM a maggiore ingrandimento delle regioni di frattura di schianto per i corrispondenti provini AB, HIP e HIPT6.*

Although the HIP condition exhibited the lowest yield and ultimate tensile strengths, it substantially improved fatigue resistance by reducing the defects that drive crack initiation. The HIPT6 condition restored the strength of the alloy through precipitation hardening while preserving the benefits of defect reduction achieved by HIP, resulting in the highest fatigue limit. These findings demonstrate that, for L-PBF AlSi10Mg alloy, fatigue performance is governed primarily by the interplay between defect population and microstructural evolution rather than by static tensile strength alone. The fracture surface observations consistently support this interpretation, showing a transition from defect-assisted crack initiation in the AB condition to crack initiation from much smaller discontinuities after post-processing, together with increasingly ductile overload fracture. Consequently, the results highlight a coherent mechanism that directly links microstructural evolution, tensile properties and fatigue behaviour of the post-treated alloy when compared with the AB condition.

CONCLUSIONS

In this study, the effects of hot-isostatic pressing (HIP) and an integrated HIP-T6 treatment (HIPT6) on the tensile and rotating-bending fatigue performance of L-PBF AlSi10Mg alloy were investigated. Based on the results, the following conclusions can be drawn:

- AB specimens exhibited the highest UTS but limited ductility and the lowest fatigue limit due to the peculiar microstructure characterized by a cellular dendritic Al-Si eutectic network and the presence of process-induced defects.
- The HIP treatment strongly improved the fatigue limit by reducing internal porosity, despite it also reduced tensile strength due to the disruption of the Al-Si eutectic network and coarsening of Si particles.
- The HIPT6 treatment provided the most balanced mechanical performance; precipitation hardening restored the tensile strength and achieved the highest fatigue limit.
- Fractography confirmed a transition from a defect from defect-assisted crack initiation in the AB condition to initiation at minor surface discontinuities in the HIP and HIPT6 conditions, with the latter showing highly ductile overload regions dominated by microvoid coalescence.

ACKNOWLEDGMENTS

The research study was conducted with the financial support of the PR-FESR EMILIA ROMAGNA 2021-2027 program through the ALERT project (Leghe di alluminio per componenti soggetti a fatica e fretting: Rivestimenti e trattamenti superficiali integrati).

REFERENCES

[1] Sefene E.M., State-of-the-art of selective laser melting process: a comprehensive review, J Manuf Syst., 2022;63:250-274. doi:10.1016/j.jmsy.2022.04.002.
[2] Zhu Z., Hu Z., Seet H.L., Liu T., Liao W., Ramamurty U. et al., Recent progress on the additive manufacturing of aluminum alloys and aluminum matrix composites: microstructure, properties, and applications, Int J Mach Tools Manuf., 2023;190:104047. doi:10.1016/j.ijmachtools.2023.104047.
[3] Tan Q., Zhang M., Recent advances in inoculation treatment for powder-based additive manufacturing of aluminium alloys, Mater Sci Eng R Rep., 2024;158:100773. doi:10.1016/j.mser.2024.100773.
[4] Ramavajjala A.K., Dandekar T.R., Khatirkar R.K., Joshi C., Chouhan R.N., Agnihotri A., A review on the correlation between microstructure, heat treatment and mechanical properties of additively manufactured AlSi10Mg by LPBF, Crit Rev Solid State Mater Sci., 2024;50(3):239-274. doi:10.1080/10408436.2024.2414012.
[5] Hyer H., Zhou L., Park S. et al., Understanding the laser powder bed fusion of AlSi10Mg alloy, Metallogr Microstruct Anal., 2020;9:484-502. doi:10.1007/s13632-020-00659-w.
[6] Sausto F., Carrion P., Shamsaei N., Beretta S., Fatigue failure mechanisms for AlSi10Mg manufactured by L-PBF under axial and torsional loads: The role of defects and residual stresses, Int J Fatigue, 2022;159:106798.
[7] Uzan N.E., Shneck R., Yeheskel O., Frage N., Fatigue of AlSi10Mg specimens fabricated by additive manufacturing selective laser melting (AM-SLM), Materials Science and Engineering: A, 2017 Sep 17;704:229-37.
[8] Brandl E., Aversa A., Bongiovanni R., Campana G., Casalino G., Fanesi A. et al., Improving the fatigue behaviour of a selectively laser melted aluminium alloy: Influence of heat treatment and surface quality, Materials & Design, 2016;104:174-182.
[9] Cova M., Tovo R., Fitting fatigue data with a bi-conditional model, Fatigue Fract Eng Mater Struct., 2017;40:732-748.

Ottimizzazione delle proprietà a fatica della lega AlSi10Mg L-PBF tramite post-processo integrato HIP e T6

Il processo di fusione laser a letto di polvere (L-PBF) consente la fabbricazione di componenti complessi in lega AlSi10Mg per applicazioni strutturali leggere. Tuttavia, lo stato "as-built" (AB) presenta difetti indotti dal processo e anisotropia microstrutturale che ne riducono le prestazioni a fatica. Lo studio indaga l'influenza di due post-trattamenti – la pressatura isostatica a caldo (HIP) e l'HIP integrato con il trattamento termico T6 (HIPT6) – sulla microstruttura e sul comportamento a fatica a flessione rotante (fino a $5X10^6$ cicli) della lega AlSi10Mg. Le relative curve S-N sono state stimate tramite un modello probabilistico bi-condizionale (P-S-N) di letteratura. I risultati mostrano che l'HIP riduce drasticamente i difetti interni, aumentando la resistenza a fatica in regime a medio-alto numero di cicli. Sebbene lo stato HIPT6 mostri una maggiore dispersione statistica della durata a fatica rispetto ad AB e HIP, esso offre prestazioni superiori ad ampiezze di sforzo elevate. I meccanismi di frattura sono stati studiati mediante indagini frattografiche condotte in microscopia elettronica a scansione (SEM).

PAROLE CHIAVE: ALSI10MG; TRATTAMENTI TERMICI POST-FABBRICAZIONE; PROVE DI FATICA A FLESSIONE ROTANTE; MICROSTRUTTURA.

TORNA ALL'INDICE >